Hollow-core photonic bandgap fiber polarizer

H. F. Xuan,[1,2] W. Jin,[1,*] J. Ju,[1] Y. P. Wang,[1] M. Zhang,[2] Y. B. Liao,[2] and M. H. Chen[2]

[1]*Department of Electrical Engineering, The Hong Kong Polytechnic University, Hong Kong, China*
[2]*Department of Electronic Engineering, Tsinghua University, Beijing 100084, China*
**Corresponding author: eewjin@polyu.edu.hk*

Received January 3, 2008; revised February 25, 2008; accepted March 7, 2008;
posted March 12, 2008 (Doc. ID 91367); published April 14, 2008

Broadband, compact in-fiber polarizers were fabricated using a pulsed CO_2 laser to modify the air holes along one side of the hollow-core photonic bandgap fibers. The polarizers have lengths from 3 to 6 mm and exhibit a polarization extinction ratio of better than 20 dB over a wavelength range larger than 100 nm at approximately 1550 nm. © 2008 Optical Society of America

OCIS codes: 060.5295, 060.2340, 130.5440.

Fiber-optic polarizers and polarizing devices are important elements in optical fiber sensors and communication systems. Compared to their bulk counterparts, in-fiber polarizers have the advantages of easier alignment, smaller insertion loss, and full compatibility with optical fiber systems. Conventional in-fiber polarizers are based on the side-polished fibers and D-shaped fibers coated with an extra material on the flat side [1,2]. In-fiber polarizers based on 45° tilted fiber Bragg gratings are also reported [3]. We have recently found that a long-period grating written on a solid-core index-guiding photonic crystal fiber could also act as a polarizer; however, the device suffers from a narrow operational wavelength range (~10 nm) and a high insertion loss [4].

Air–silica hollow-core photonic bandgap (HC-PBG) fibers, since their first demonstration of single-mode light guiding in 1999 [5], have significantly advanced over the past several years [6,7]. Practical HC-PBG fibers with a loss as low as 1.2 dB/km have recently been reported [8]. The guiding of light in air (or vacuum) has several advantages, such as lower Rayleigh scattering, reduced nonlinearity, novel dispersion characteristics, lower phase sensitivity to ambient temperature [9], and potentially lower transmission loss than conventional fibers. These properties are expected to be beneficial to both telecommunication and sensor systems. However, to our knowledge, fiber components that are popularly used in optical fiber systems are not yet available in the form of HC-PBG fibers.

In this Letter, we report a compact HC-PBG fiber polarizer fabricated by using a pulsed CO_2 laser to modify the air holes along one side of a HC-PBG fiber. The partial collapse of air holes on one side of the fiber results in an asymmetric waveguide structure in which one polarization leaks out while the orthogonal polarization remains propagating along the fiber with relatively low loss. The fabrication, characterization, and modeling of such HC-PBG fiber polarizers are reported in the following sections.

Figure 1 shows the experimental setup for fabricating the in-fiber polarizers. An Agilent 81910A photonic all parameter analyzer is utilized to monitor online the evolution of polarization-dependent loss (PDL) during the fabrication process. The HC-PBG fiber used was purchased from Crystal Fiber A/S with its scanning electron microscope (SEM) micrograph of the fiber cross section shown in Fig. 2(a). The HC-PBG fiber was spliced to Corning SMF-28 pigtail fibers at both ends, with one pigtail connected to the tunable laser module with an adjustable polarization state and the other pigtail was connected to the photodetection module to record the wavelength-dependent PDL. The CO_2 laser emits pulses with a width of 2.0 μs, a repetition rate of 10 kHz, and an average power of ~0.2 W. The CO_2 beam is focused to a spot size of ~35 μm and can be scanned, via a computer controlled two-dimensional optical scanner, transversely and longitudinally as instructed by the computer program. During the fabrication, the laser beam is first scanned transversely across the fiber and then moved longitudinally by a step of $\Lambda = 30$ to 50 μm, and then another transverse scan is repeated. This procedure is repeated for N times until a desired longitudinal movement of $L = N\Lambda$ is reached. This whole process of making N successive transverse scans is called one scanning cycle. The high-frequency CO_2 laser pulses hit repeatedly on one side of the PBG fiber, for each transverse scan, and induce a local high temperature around a point along the surface of the fiber. This causes glass ablation on the surface and also a change in the shape, size, location, and even the complete collapse, of some of the air holes in the cladding, which creates a notch on the surface of the fiber. The N successive transverse scans (i.e., one scanning cycle) create N closely spaced notches, which form a broad valley along the fiber surface with a dimension (device length) of approximately $L = N\Lambda$. The depth of the valley resulting

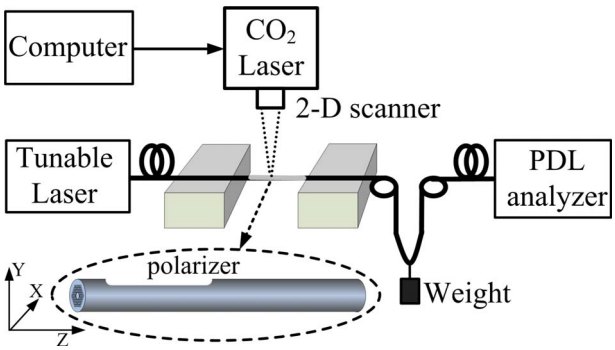

Fig. 1. (Color online) Experimental setup for polarizer fabrication.

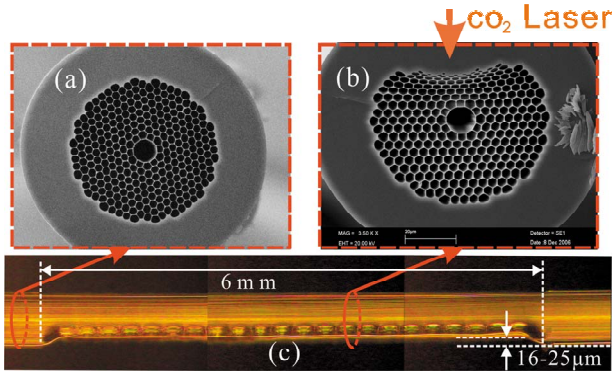

Fig. 2. (Color online) (a) SEM image of the original HC-1550-02 PBG fiber. (b) Cross section and (c) side view of valley created by CO_2 laser irradiation. Only segments of the valley are shown in (c).

from one scanning cycle is determined by the power of the pulses, and a deeper valley is created by having more scanning cycles. Figures 2(b) and 2(c) show the cross section and the side view, respectively, of a typical valley created after 28 scanning cycles.

Figure 3 shows the evolution of wavelength-dependent PDL for a different number of scanning cycles. The PDL of the original HC-1550-02 fiber is very low (<0.05 dB/m) and increases with the number of scanning cycles. After 31 scanning cycles, a PDL or extinction ratio of above 30 dB over a wavelength of wider than 50 nm (from 1570 to 1620 nm) is achieved. After 39 scanning cycles, the PDL is above 23 dB over a wavelength of more than 100 nm (from below 1520 to 1620 nm). The insertion loss of the device also depends on the number of scanning cycles. For 26, 31, and 39 scanning cycles, the insertion losses are estimated to be, respectively, from below 1 to 1.8 dB, 3 to 4 dB, and 5.5 to 7 dB over the wavelength range from 1520 to 1620 nm.

The performance (maximum PDL, wavelength range, and insertion loss) of the polarizer is affected by the dimension (the CO_2 laser treated region or device length) and the depth of the valley. The device length is approximately determined by the number of transverse scans and the longitudinal steps between each scan. The depth is associated with the collapse

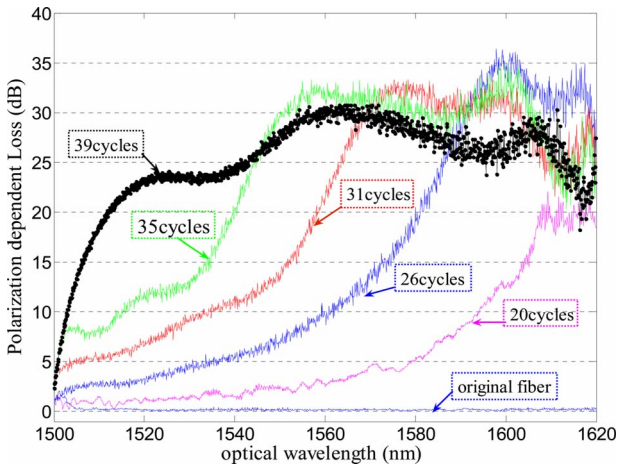

Fig. 3. (Color online) Evolution of PDL with the number of CO_2-laser-scanning cycles.

of air holes and is affected by the average power of CO_2 laser pulses and the number of scanning cycles. For the same device length, large PDL may be achieved by a deeper valley; however, the insertion loss may become excessive if the depth is beyond a certain value (e.g., 25 μm). The average power of CO_2 laser pulses affects the depth of the valley created in one scanning cycle, which has a great influence on insertion loss. Generally, high-average energy pulses may cause high insertion loss, while a lower-average energy pulse with more scanning cycles may realize a low-loss polarizer with sufficient PDL. The device length and flatness of the valley are two other important factors. Longer length with reasonable depth results in a higher PDL with acceptable insertion loss for the guided polarization mode. Our experimental investigations show that 1 mm length may be the lower limit to achieve sufficient PDL but with a still reasonable insertion loss. Although further investigation is still needed, the unevenness of the periodic notches that form the valley might be the reason behind the fringelike fluctuation in the PDL curve as shown in Fig. 3. The periodic unevenness might excite higher-order modes, and multimode interference might cause these fluctuations. The unevenness may be improved by modifying the fabrication procedure, for example, by introducing a shift (longitudinal displacement) of $\Lambda/2$ in alternative scanning cycles. It is believed that by optimizing the device length, the fabrication parameters, and the procedure, better performance polarizers may be produced.

The polarization property of the HC-PBG fiber polarizer was further investigated by using the Profile Opcische System PAT9000B kit. The PAT9000B kit can be programmed to produce linearly polarized light at different wavelengths, and polarization direction can be rotated from 0° to 360°. The degree of polarization of the linearly polarized light is at least 99.8% for every polarization direction. The normalized transmitted output light power from a 3 mm length HC-PBG polarizer as a function of input polarization direction is shown in Fig. 4(a). As expected, the output of the polarizer has two maxima and minima for a 360° rotation of the input polarization direction. For this particular measurement, the output has peaks located at 25° and 205° and has almost

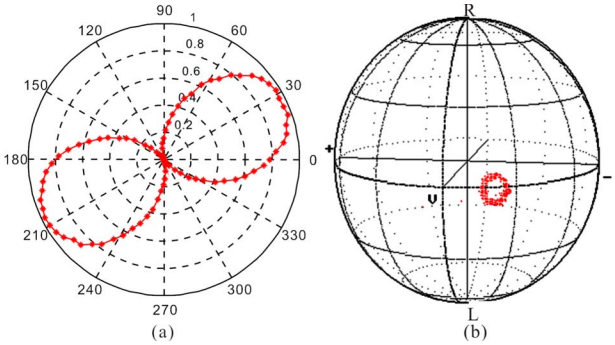

Fig. 4. (Color online) (a) Response of a 3 mm HC-PBG fiber polarizer to linearly polarized light at 1550 nm with direction varying from 0° to 360°, (b) trace of output polarization state on the Poincare sphere when the input light is evolving from left to right circular polarization.

zero outputs at orthogonal directions. This indicates that the output from the polarizer is indeed linearly polarized.

The PAT9000B kit also allows the polarization state of transmission light to be traced on the Poincare sphere when the input polarization state evolves arbitrarily and repeatedly from left circularly, through elliptically and linearly, to right circularly polarized light. The trace for the 3 mm length polarizer is shown in Fig. 4(b). The output light of this polarizer remains approximately linearly polarized regardless the state of input polarization.

To understand the reasons behind the large PDL over the broad wavelength range, we calculated the mode field distributions and the confinement losses of the two principal polarization states for the two model structures shown in Figs. 5(a) and 5(b). Figure 5(a) is a simplified structure with the following structural parameters: the spacing between the holes is $\Lambda = 3.8\ \mu$m, the relative hole diameter $d/\Lambda \approx 0.96$, and the air filling fraction ≈90%. Figure 5(b) is a model structure that resembles the real structure as shown in Fig. 2(b). A full-vector finite-element method with perfectly matched layers [10,11] was used to analyze the model structures, and the mode fields of the two orthogonal polarizations at 1580 nm are shown in the insets in Figs. 5(a) and 5(b). Obviously the model fields of the y polarization are not so well confined as compared to the x polarizations. The calculated confinement losses of the y polarizations are significantly larger than that of the x polarizations over the wavelength range from 1500 to 1620 nm.

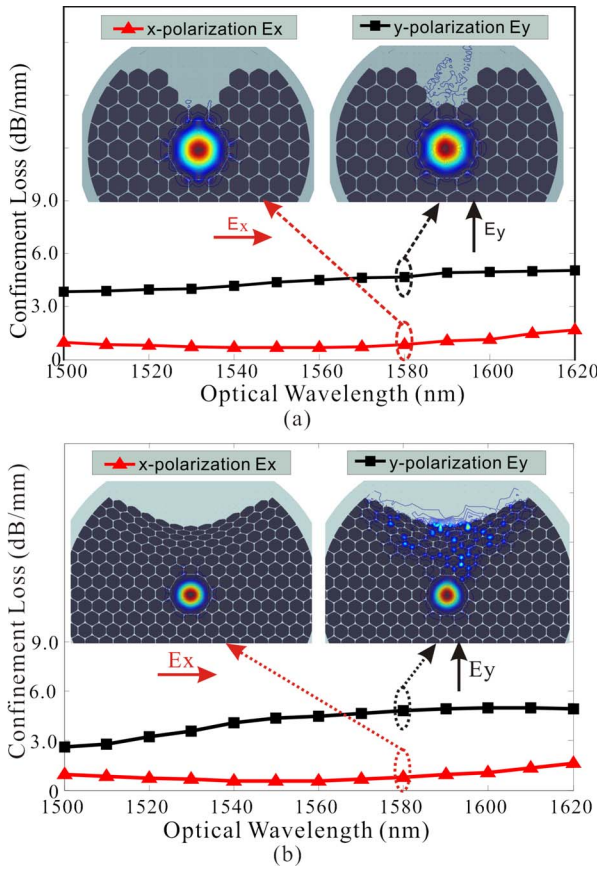

Fig. 5. (Color online) Calculated confinement losses of two orthogonal polarizations as functions of wavelength. (a) A simplified model, and (b) a model that resembles the SEM image in Fig. 2(b).

From the above analysis, we may conclude that the deformation of air holes on one side of the cladding region is responsible for the high PDL observed. The deformation of air holes on one side of the cladding results in an asymmetric waveguide structure that leads to significant leakage of one polarization, while the orthogonal polarization remains propagating along the waveguide with relatively low loss. The slight deformation of the hollow core as shown in Fig. 2(b) enhances the waveguide asymmetry and may also contribute to the PDL observed. Further detailed theoretical modeling and experimental investigation may help us to better understand the polarization behavior of the deformed hollow-core PBG fibers and hence to optimize the performance of polarizers based on such fibers.

In conclusion, novel broadband, compact all-fiber polarizers were fabricated by using CO_2 laser pulses to modify the air holes along one side of the hollow-core photonic bandgap (HC-PBG) fibers. These polarizers have extinction ratios from 20 to beyond 30 dB over a wavelength range from 50 to 110 nm. More detailed theoretical and experimental investigations on the mechanisms responsible for the large polarization dependent loss and on the effects of varying hole size, shape, and distribution on the polarizer performance are ongoing. Polarizers with better performance could be realized by optimizing fabrication parameters.

This work was supported by the Hong Kong SAR government through a CERG grant PolyU 5243/04E and the NSFC of China through a grant 60629401. We thank Q. Lin of Beijing Institute for Glass Research for his technical support.

References

1. R. A. Bergh, H. C. Lefevre, and H. J. Shaw, Opt. Lett. **5**, 479 (1980).
2. R. B. Dyott, J. Bello, and V. A. Handerek, Opt. Lett. **12**, 287 (1987).
3. K. M. Zhou, G. Simpson, X. F. Chen, L. Zhang, and I. Bennion, Opt. Lett. **30**, 1285 (2005).
4. Y. P. Wang, L. M. Xiao, D. N. Wang, and W. Jin, Opt. Lett. **32**, 1035 (2007).
5. R. F. Cregan, B. J. Mangan, J. C. Knight, T. A. Birks, P. S. Russell, P. J. Roberts, and D. C. Allan, Science **285**, 1537 (1999).
6. C. M. Smith, N. Venkataraman, M. T. Gallagher, D. Muller, J. A. West, N. F. Borrelli, D. C. Allan, and K. W. Koch, Nature **424**, 657 (2003).
7. J. C. Knight, Nature **424**, 847 (2003).
8. P. J. Roberts, F. Couny, H. Sabert, B. J. Mangan, D. P. Williams, L. Farr, M. W. Mason, A. Tomlinson, T. A. Birks, J. C. Knight, and P. S. J. Russell, Opt. Express **13**, 236 (2005).
9. V. Dangui, H. K. Kim, M. J. F. Digonnet, and G. S. Kino, Opt. Express **13**, 6669 (2005).
10. K. Saitoh and M. Koshiba, IEEE Photon. Technol. Lett. **15**, 236 (2003).
11. S. Selleri, L. Vincetti, A. Cucinotta, and M. Zoboli, Opt. Quantum Electron. **33**, 359 (2001).